**Porphyrazines**
Порфиразины

*Макрогетероциклы*
http://macroheterocycles.isuct.ru

**Paper**
Статья

# Thiadiazole Fused Subporphyrazines as Acceptors in Organic Photovoltaic Cells

Georgy L. Pakhomov,[a,b] Vlad V. Travkin,[a] Mahmoud Hamdoush,[b] Yuriy A. Zhabanov,[b] and Pavel A. Stuzhin[b@]

Dedicated to Academician Aslan Yusupovich Tsivadze on the occasion of his Birthday

[a]*Institute for Physics of Microstructures of the Russian Academy of Sciences (IPM RAS), 603905 Nizhny Novgorod, Russian Federation*
[b]*Institute of Macroheterocycles, Ivanovo State University of Chemistry and Technology (ISUCT), 153000 Ivanovo, Russian Federation*
[@]*Corresponding author E-mail: stuzhin@isuct.ru*

*A series of archetypal photovoltaic cells with a fully-subporphyrinoid planar heterojunction was fabricated by the thermal vacuum evaporation technique. The donor component of this junction was a boron subphthalocyanine chloride, while the acceptor component was perfluorinated subphthalocyanine or its heterocyclic analogues in which one, two or three tetrafluorobenzene ring(s) were substituted by the 1,2,5-thiadiazole ring(s) using the recently described synthetic approach. The photovoltaic parameters of such cells were measured and compared to those of the reference cell with the conventional fullerene $C_{60}$ as electron acceptor.*

**Keywords:** Subphthalocyanines, perfluorinated and 1,2,5-thiadiazole fused analogues, subporphyrazines, thin films, molecular heterojunctions, photovoltaic cells, open circuit voltage.

# Тиадиазол–аннелированные субпорфиразины как акцепторы в органических фотовольтаических ячейках

Г. Л. Пахомов,[a,b] В. В. Травкин,[a] М. Хамдуш,[b] Ю. А. Жабанов,[b] П. А. Стужин[b@]

[a]*Институт физики микроструктур Российской Академии Наук, 603950 Нижний Новгород, Россия*
[b]*НИИ Макрогетероциклических соединений, Ивановский государственный химико-технологический университет, 153000 Иваново, Россия*
[@]*E-mail: stuzhin@isuct.ru*

*Была изготовлена серия модельных фотовольтаических ячеек на основе полностью субпорфириноидного планарного гетероперехода, сформированного методом термовакуумного испарения. Донорным компонентом этого гетероперехода был обычный незамещенный субфталоцианинатобор(III) хлорид, а акцепторным компонентом – перфторированный субфталоцианин или его гетероциклические аналоги, в которых один, два или все три тетрафторбензольных фрагмента были замещены на 1,2,5-тиадиазольный цикл. Были измерены основные параметры фотопреобразования и проведено их сравнение с параметрами аналогичных ячеек, в которых использовался традиционный акцептор – фуллерен $C_{60}$.*

**Ключевые слова:** Субфталоцианины, перфторированные и 1,2,5-тиадиазол-аннелированные аналоги, субпорфиразины, тонкие плёнки, молекулярные гетеропереходы, фотовольтаические ячейки.

## Introduction

Halogen-substituted subphthalocyanines (SubPc) attracted much attention as electron acceptors in so-called 'fullerene-free' photovoltaics, including devices with all subphthalocyanine-based[12-3] and cascade junctions[4] (see also reviews by Torres *et al.*[5] and Bender *et al.*[6]). Parent compound, unsubstituted subphthalocyaninatoboron(III) chloride is routinely utilized as a donor in the devices containing molecular[5,6] or hybrid[7] heterojunctions, but can also serve as an acceptor in conjunction with the electron-rich molecular materials, such as polyarenes or thiophenes.[8] It was recently shown that even without *p/n* junction subphthalocyanines give higher yields of free charge carriers upon photoexcitation than other molecular semiconductors.[3]

Fusion of 1,2,5-thiadiazole rings strongly enhances the π-electron-deficiency of the porphyrazine macrocycle[9,10] allowing to use tetra(1,2,5-thiadiazolo)porphyrazine and its metal complexes as *n*-type organic semiconductors in prototypes of the field-effect transistors[11] and in photovoltaic cells as acceptors instead of fullerene.[12]

We have synthesized novel heterocyclic subphthalocyanine analogue – subporphyrazine bearing three fused 1,2,5-thiadiazole rings[13] and, very recently, two low-symmetry analogues of perfluorinated subphthalocyanine having 1,2,5-thiadiazole ring(s) instead of one or two benzene rings.[14] These subporphyrazines form together with symmetrical subphthalocyanines a series of cognate subporphyrinoids as shown in Chart 1. The first three compounds of this series formally belong to the family of 1,2,5-thiadiazole fused subporphyrazines, in which peripheral 1,2,5-thiadiazole unit is consecutively replaced with the four-fold fluorinated benzene ring. These are denoted as $SubPzS_3F_0$, $SubPzS_2F_4$ and $SubPzS_1F_8$ (Chart 1). Naturally, the ultimate stage of such a replacement leads, using the given abbreviation format, to $SubPzS_0F_{12}$, *i.e.*, the well-known chloro[dodecafluorosubphthalocyaninato]boron(III), frequently termed as perfluorinated-SubPc. Following the existing tradition[1,2,5,6,15,16] this compound is denoted as $SubPcF_{12}$ in Chart 1.

Judging from the molecular structures[15,17] and our DFT calculation results (Figure 1), the first four compounds in Chart 1 should behave as electron acceptors at the molecular level and as *n*-type semiconductors in the solid state. In this work, we have employed them as electron-transporting and acceptor components in the archetypal thin-film photovoltaic cells with a planar molecular heterojunction. Another (donor) component was unsubstituted subphthalocyaninatoboron(III) chloride, also termed as per-
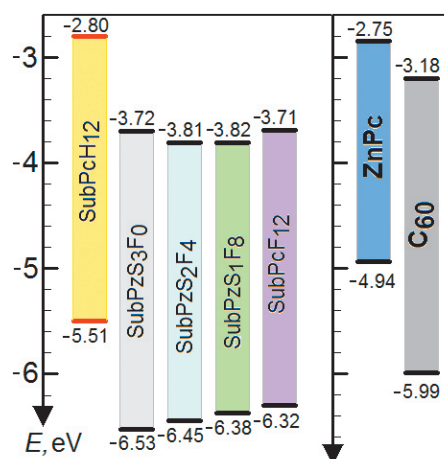


**Figure 1.** Positions of highest occupied and lowest unoccupied molecular orbitals (HOMO and LUMO) of complexes from Chart 1 obtained from DFT B3LYP calculations (left panel). For comparison, the calculated HOMO-LUMO gaps for the conventional donor, zinc phthalocyanine ZnPc, and acceptor, fullerene $C_{60}$ (from ref.[16]) are shown in the right panel.

hydrogenated-SubPc[16] (fifth compound in Chart 1, denoted as $SubPcH_{12}$), so that the fully subporphyrinoid-based heterojunctions were obtained.

## Experimental

The synthetic routes and related procedures (purification, identification) are described in the preceding works.[13,14]

The preparation of the archetypal photovoltaic cell was similar to that previously reported.[18,19] The cell scheme was 'glass/ITO/MoOₓ/SubPcH₁₂/acceptor/Al', where $MoO_x$ is a 10 nm substoichiometric molybdenum trioxide layer (buffer/workfunction modifier,[1,5-8,19] see Figure S1), acceptor = $SubPzS_3F_0$, $SubPzS_2F_4$, $SubPzS_1F_8$, $SubPcF_{12}$ (or $C_{60}$, see text), and Al is an aluminum top cathode (40 nm). The thickness of a *p*-type layer ($SubPcH_{12}$) was 20 nm, the thickness of an *n*-type (acceptor) layer was 30 nm. All functional layers were obtained by the thermal evaporation technique,[15,16,18,19] the standard Aldrich ITO-coated glass slides were used as substrates. (Photo-)electrical characterization of the cells with an active area of 0.16 cm² was carried out in an inert atmosphere (argon) at the room temperature using a Zolix SS150 solar simulator and a Keithley 4200 SCS parameter analyzer. Data are presented in Table 1, Figure 2 and in Supporting Information (Figures S1-S3).
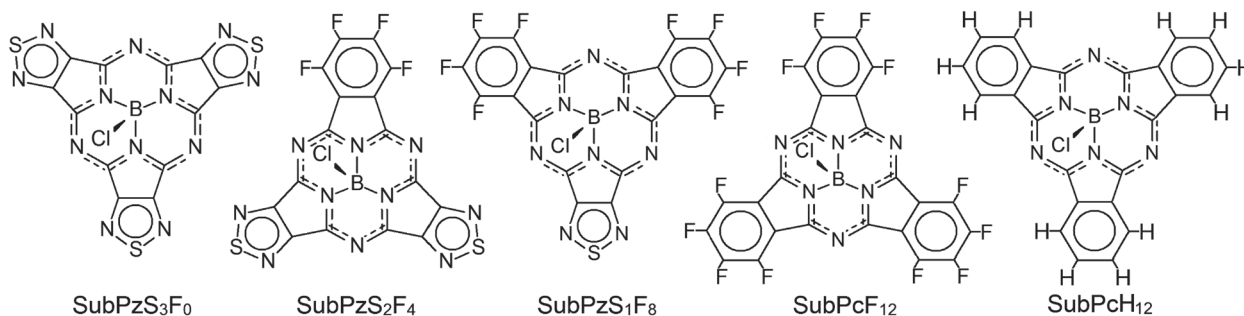


**Chart 1.** Molecular structures.

The energy of the frontier molecular orbitals for the subporphyrinoids presented in Chart 1 was estimated by quantum chemical calculations using the density functional theory method (B3LYP functional with all electron pcseg-2 basis sets[20]). The detailed discussion of the calculation results will be published elsewhere.

## Results and Discussion

Dark $J$-$V$ dependences for the cells with the all-subporphyrinod heterojunctions are shown in Figure 2a-d. The rectification in the darkness is usually poor, most likely due to compensating (unwanted) contribution of the interactive 'acceptor/Al' junction.[1-3,18,19] Under illumination of 100 mW/cm², a photovoltaic effect arises (Figure 2(a-d)), the corresponding parameters are summarized in Table 1. Significant photovoltage generated by the molecular heterojunction can be expected from the large difference between HOMO energy of donor (SubPcH$_{12}$) and LUMO energy of acceptor (see Figure 1). These values are obtained from the B3LYP DFT calculations (pcseg-2[20] basis sets) and should be treated with care when comparing to other sources.[1,6,21] They do represent only the relative positions of the energy levels in the series of subporphyrinoids used in this work. The highest $U_{oc}$ value in this series was measured on the cells containing SubPcF$_{12}$ as acceptor, but the best performing cell contains SubPzS$_1$F$_8$. The latter provides the maximal value of short circuit current $J_{sc}$ contributing to the overall cell efficiency (see Table 1).

Fill factors in such cells typically suffer from the high parasitic resistances, basically serial resistance $R_s$, and from

the limited charge extraction at the cathode[1] (see, *e.g.* Figure 2(f)). Note that the layer thicknesses were not optimized for each particular materials combination, instead, we intended to maintain the equality of the cell scheme for the sake of appropriate comparison.[22] For the same reason, the 'acceptor/cathode' interface was not modified by insertion of the exciton blocking and/or electron transporting layers. As known, an exciton-blocking material should carefully be adapted for the specific acceptor/cathode pair to avoid substantial energy losses at the interface.[1-3,6,8,18,19,22] An indirect argument for this is the lack of correlation between the value of $U_{oc}$ (Table 1) and the LUMO position in acceptor (Figure 1).

This is illustrated in Figure 2(f). When an 8 nm thick layer of a wide bandgap bathocuproine (BCP) is inserted, both the photovoltage and photocurrent increase in the cell with the SubPcF$_{12}$ acceptor (by 0.07 V and 0.022 mA/cm², respectively). However, for the SubPzS$_3$F$_0$-based cell, insertion of BCP leads to the much greater increase in $U_{oc}$ (up to 1.25 V), while $J_{sc}$ decreases by a factor of five. Next, although rectification in the darkness is improved by BCP (Figure S2), insertion of a highly resistive BCP interlayer adds to $R_s$, and a 'kink'[1] appears in the 4th quadrant of illuminated $J$-$V$ plot – Figure 2(f). Therefore, this approach cannot be automatically applied to the 'subporhyrazine/metal' interface and requires a more detailed study (to be published later).

As it is seen from Figure 2(b,c), the devices with low symmetry compounds are more effective in the photoconductive mode than in the photovoltaic mode, *i.e.*, behave rather as photodiodes. The photocurrent signals $S^{photo}$ at 1 V reverse bias (marked by arrows in Figure 2(a-e)) are listed
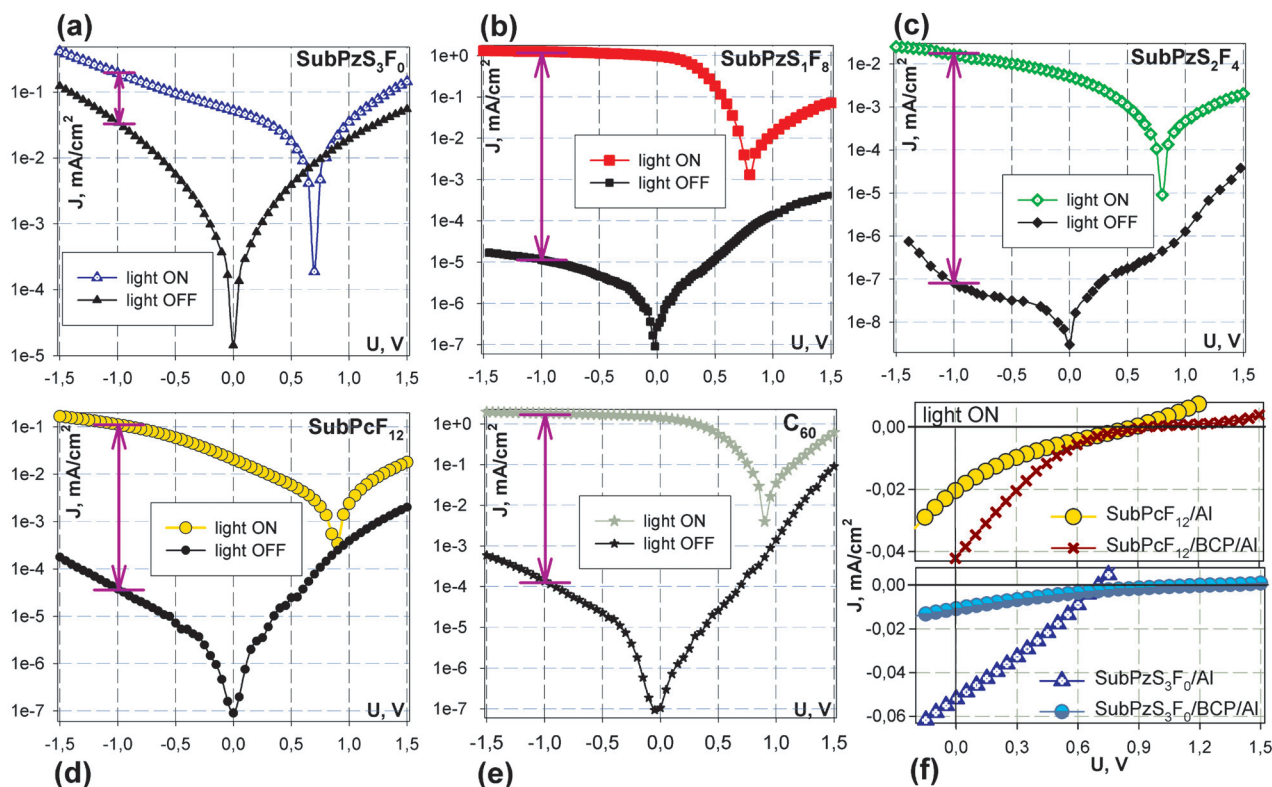


**Figure 2.** $J$-$V$ characteristics of the glass/ITO/MoO$_x$/SubPcH$_{12}$/acceptor/Al cells, where acceptor = SubPzS$_3$F$_0$, SubPzS$_2$F$_4$, SubPzS$_1$F$_8$, SubPcF$_{12}$ or C$_{60}$ (a-e); and 4th quadrant of linear $J$-$V$ plot for the illuminated SubPzS$_3$F$_0$- and SubPcF$_{12}$-based cells with and without BCP under anode (f).

**Table 1.** Parameters of the cells with a 'SubPcH$_{12}$/acceptor' heterojunction, acceptor = SubPzS$_3$F$_0$, SubPzS$_2$F$_4$, SubPzS$_1$F$_8$, SubPcF$_{12}$ or C$_{60}$. $U_{oc}$ = open circuit voltage, $J_{sc}$ = short circuit current.

|  | SubPzS$_3$F$_0$ | SubPzS$_2$F$_4$ | SubPzS$_1$F$_8$ | SubPcF$_{12}$ | C$_{60}$ |
|---|---|---|---|---|---|
| $U_{oc}$, V | 0.70 | 0.80 | 0.80 | 0.89 | 0.90 |
| $J_{sc}$, mA/cm$^2$ | 0.05 | $5 \cdot 10^{-3}$ | 0.98 | 0.02 | 1.43 |
| S$^{photo*}$ | 6 | $2.0 \cdot 10^5$ | $1.1 \cdot 10^5$ | $2.9 \cdot 10^3$ | $1.0 \cdot 10^4$ |

\* S$^{photo}$ = photocurrent signal, determined as photo-to-dark current ratio at –1 V (see, Figure 2(a-e)).

in Table 1. Notably, specific conductivities of the thick films of subporphyrazines are very low, in order of $10^{-11}$ Ohm$^{-1} \cdot$cm$^{-1}$ (measured in the planar cells with symmetrical interdigital contacts). Differences in the dark currents leaking vertically through the sandwich-type cells can be caused by the different packing of molecules (densities, void fractions[16]), which determines the conductive pathways in the ultrathin vacuum deposited layers. Under illumination, the photogeneration and field-assisted transport of charge carriers is quite intensive, for example in case of the SubPcH$_{12}$/SubPzS$_2$F$_4$ heterojunction S$^{photo}$ is as high as $2.0 \cdot 10^5$ (Table 1).

It is interesting to compare the measured parameters with those of the equivalent cells, in which another, well-known and effective, acceptor is employed, *e.g.*, fullerene.[1,2,4,8,18,22] Therefore, as a reference, we used similarly made cells incorporating a SubPcH$_{12}$/C$_{60}$ junction, with the same scheme and layer thickness as in all subporphyrinoid-based cells (Figure 2(e)).

As it is seen from Table 1, the reference cell incorporating the SubPc/C$_{60}$ heterojunction shows better parameters than any cell with the subporphyrinoid as acceptor, except for the S$^{photo}$ value. Despite a severe 'kink' induced by the unmodified C$_{60}$/Al interface (Figure 2(e)), the high charge carrier mobility and, probably, appropriate positions of molecular energy levels in fullerene allow for better performance of the reference cell.[4,22]

## Conclusion

In the archetypal photovoltaic cells with planar molecular heterojunction, the newly synthesized subporphyrazines SubPzS$_3$F$_0$, SubPzS$_2$F$_4$, and SubPzS$_1$F$_8$ behave as effective acceptors when paired with a sister SubPcH$_{12}$ compound. Low symmetry derivatives SubPzS$_2$F$_4$ and SubPzS$_1$F$_8$ are excellent photoconductors, and yield photovoltage comparable to that obtained with such well-known acceptors as SubPcF$_{12}$ or C$_{60}$. However, the unbalanced charge transport through the cells incorporating these derivatives and their high layer resistance deteriorate the output parameters. Optimization of the thickness and introduction of the charge transporting interlayers are the possible ways to maximize the cell efficiency. Therefore, we believe that the subporphyrazine-type compounds described here, thanks to their low sublimation temperatures, stability and high absorption coefficients in visible range, have good potential as alternative to C$_{60}$ for use in the organic photovoltaics.

## References

1. Cnops K., Zango G., Genoe J., Heremans P., Martinez-Diaz M.V., Torres T., Cheyns D. *J. Am. Chem. Soc.* **2015**, *137*, 8991−8997.
2. Gommans H., Aernouts T., Verreet B., Heremans P., Medina A., Claessens Ch.G., Torres T. *Adv. Funct. Mater.* **2009**, *19*, 3435–3439.
3. Chandran H.T., Ng T.-W., Foo Y., Li H.-W., Qing J., Liu X.-K., Chan C.-Y., Wong F.-L., Zapien J.A., Tsang S.-W., Lo M.-F., Lee C.-S. *Adv. Mater.* **2017**, *29*, 1606909.
4. Cnops K., Rand B.P., Cheyns D., Verreet B., Empl M.A., Heremans P. *Nat. Commun.* **2014**, *5*, 3406.
5. Claessens Ch.G., González-Rodríguez D., Rodríguez-Morgade M.S., Medina A., Torres T. *Chem. Rev.* **2014**, *114*, 2192–2277.
6. Morse G.E., Bender T.P. *ACS Appl. Mater. Interfaces* **2012**, *4*, 5055−5068.
7. Dearden C.A., Walker M., Beaumont N., Hancox I., Unsworth N.K., Sullivan P., McConville C.F., Jones T.S. *Phys. Chem. Chem. Phys.* **2014**, *16*, 18926−18932.
8. (a) Beaumont N., Cho S.W., Sullivan P., Newby D., Smith K.E., Jones T.S. *Adv. Funct. Mater*. **2012**, *22*, 561–566; (b) Beaumont N., Castrucci J.S., Sullivan P., Morse G.E., Paton A.S., Lu Z.-H., Bender T.P., Jones T.S. *J. Phys. Chem. C* **2014**, *118*, 14813−14823.
9. Donzello M.P., Ercolani C., Stuzhin P.A. *Coord. Chem. Rev.* **2006**, *250*, 1530-1561.
10. Zhabanov Yu.A., Tverdova N.V., Giricheva N.I., Girichev G.V., Stuzhin P.A. *J. Porphyrins Phthalocyanines* **2017**, *21*, 439–452.
11. (a) Miyoshi Y., Kubo M., Fujinawa T., Suzuki Y., Yoshikawa H., Awaga K. *Angew. Chem. Int. Ed.* **2007**, *46*, 5532–5536; (b) Miyoshi Y., Fujimoto T., Yoshikawa H., Matsushita M.M., Awaga K., Yamada T., Ito H. *Org. Electron.* **2011**, *12*, 239–243.
12. Stuzhin P.A., Mikhailov M.S., Travkin V.V., Gudkov E.Y., Pakhomov G.L. *Macroheterocycles* **2012**, *5*, 162−165.
13. Hamdoush M., Ivanova S.S., Pakhomov G.L., Stuzhin P.A. *Macroheterocycles* **2016**, *9*, 230–233.
14. Hamdoush M., Skvortsov I.A., Mikhailov M.S., Pakhomov G.L., Stuzhin P.A. *J. Fluorine Chem.* **2017**, *204*, 31–36.
15. Mattheus C.C., Michaelis W., Kelting C., Durfee W.S., Wohrle D., Schlettwein D. *Synth. Met.* **2004**, *146*, 335–339.
16. Morse G.E., Gong I., Kawar Y., Lough A.J., Bender T.P. *Cryst. Growth Des.* **2014**, *14*, 2138−2147.
17. Tang M.L., Oh J.H., Reichardt A.D., Bao Zh. *J. Am. Chem. Soc.* **2009**, *131*, 3733–3740.
18. Travkin V.V., Yunin P.A., Luk'yanov A.Y., Stuzhin P.A., Pakhomov G.L. *Phys. Status Solidi A* **2017**, *214*, 1700186.
19. Travkin V.V., Stuzhin P.A., Okhapkin A.I., Korolyov S.A., Pakhomov G.L. *Synth. Met.* **2016**, *212*, 51–54.
20. Jensen F. *J. Chem. Theory Comput.* **2014**, *10*, 1074−1085.
21. Bredas J.-L. *Mater. Horiz.* **2014**, *1*, 17–19.
22. Scholz R., Luschtinetz R., Seifert G., Jageler-Hoheisel T., Korner C., Leo K., Rapacioli M. *J. Phys.: Condens. Matter* **2013**, *25*, 473201.